

# Tracking Contact Transitions During Force-Controlled Compliant Motion Using an Interacting Multiple Model Estimator

Lyudmila Mihaylova\*, Tine Lefebvre, Ernesto Staffetti, Herman Bruyninckx, Joris De Schutter

Katholieke Universiteit Leuven, Department of Mechanical Engineering  
 Celestijnenlaan 300 B, B-3001 Heverlee, Belgium, Tel. +32 16 32 25 33  
 E-mail: *Lyudmila.Mihaylova@mech.kuleuven.ac.be*

## Abstract

*This work concerns both monitoring of contact transitions and estimation of the unknown first-order geometric parameters during force-controlled motions. The robotic system is required to move an object among a sequence of contact configurations with the environment, under partial knowledge of geometric parameters (positions and orientations) of the manipulated objects and of the environment itself. An example of a compliant motion task with multiple contacts is considered, that of moving a cube into a corner. It is shown that by describing the contact configurations with different models, and by using the multiple model approach it is possible: i) to detect effectively at each moment the current contact configuration and ii) to estimate accurately the unknown parameters. The reciprocity constraints between ideal reaction forces and velocities are used as measurement equations. An Interacting Multiple Model (IMM) estimator is implemented and its performance is evaluated based on experimental data.*

**Keywords** - compliant motion, on-line estimation, IMM estimator, transition detection, tracking

## 1 Introduction

In different robot operations the manipulator has to interact with the environment through the manipulated object and modify its trajectory depending on the contact forces that arise. These force-controlled operations are called *compliant motion tasks*. Force control is required due to the fact that small errors in the models can generate high forces on the manipulator. For other tasks, such as cutting, welding or polishing, the robotic manipulator must apply a given force to execute correctly the task. In all cases the manipulator is moving an object in contact with the environment among a sequence of contact configurations.

The objects involved in compliant motion are herein supposed to be rigid and polyhedral.

The path of the manipulated object is a sequence of contact configurations. The configurations can be grouped into a subsequence of configurations equivalent from a topological point of view, i.e., in which the same elements of the manipulated object are in contact with the same elements of the environment. In this context each class of equivalence is called *contact formation* (CF) [5].

The present work assumes uncertainties in the position and orientation of both the manipulated object and the environment. In practice, besides the model uncertainties other sources of uncertainties are present as friction, burrs, sensor noises, or unexpected events. Therefore, the problem of tracking force-controlled motions is relevant and in this paper the focus is on detection of the current CF and the instant of transition between the CFs.

Encoders at the joints of the manipulator supply information about the end-effector location and motion, and a force sensor located at its wrist gives information about the forces and moments arising in the interaction with the environment. This information is used to estimate uncertain geometric parameters. In [2] a possible architecture of an autonomous assembly system is proposed. It is pointed out that such a system needs a high-level planner (responsible for planning, re-planning and on-line error recovering), a low-level module (responsible for sensing and the execution of the planned action), and a medium-level module (for estimation and monitoring).

Previous works on force-controlled compliant motion are [3, 4, 7]. In [3] the sequence of the different CFs is known and for each period a single Extended Kalman Filter (EKF) is run. The Summed Normalized Innovation Squared (SNIS) test is used as indicator of the transitions between the CFs. In [7] a solution to the estimation of the geometric parameters for one CF is proposed based on an iterated EKF. In the present work the possible CFs are described by different models and with them an Interacting Multiple Model (IMM) estimator is implemented. Its performance is investigated and evaluated by experiments

\*On leave from the Bulgarian Academy of Sciences.

with real data of different type: velocities and forces.

## 2 Problem formulation

During the compliant motion different CFs occur. They can involve, for instance, a contact between an edge of the manipulated object and a face of the environment (edge-face contact), a face of the manipulated object and a face of the environment (face-face contact), and so on (Fig. 1). To estimate the unknown geometric parameters and track the transitions between CFs, the manipulated object and the environment are considered as a stochastic hybrid system (with continuous and discrete uncertainties). The state-space equations are of the form

$$x_{k+1} = f(x_k, m_k) + g(m_k, \eta_k), \quad (1)$$

$$h_k(x_k, m_k, z_k, \xi_k) = 0, \quad (2)$$

where  $x_k \in \mathbb{R}^{n_x}$  is the system state vector, estimated based on the measurement vector  $z_k \in \mathbb{R}^{n_z}$ ;  $m_k$  is the modal state, corresponding to the CF.

The measurement equation is in implicit form, in which  $h_k$  is a function both of the estimated variables, and of the measured data  $z_k$  as in [3, 9]. The additive system and measurement noises  $\eta_k \in \mathbb{R}^{n_\eta}$  and  $\xi_k \in \mathbb{R}^{n_\xi}$  are mutually independent, white with zero mean and covariances  $Q_k$  and  $R_{z,k}$ , respectively. Functions  $f$ ,  $g$  and  $h$  are nonlinear and remain unchanged during the estimation procedure.

In this paper the focus is on detection of the current CF and the instant of transition between the CFs. The possible CFs are represented by the set

$$M = [m_1, m_2, \dots, m_N]$$

where  $m_i$  stands for the different CFs between the manipulated object and the environment. The changes between the CFs are modelled by a Markov chain with a transition probability matrix

$$Pr\{m_{j,k+1}/m_{i,k}\} = \pi_{ij,k},$$

where

$$\sum_{j=1}^N \pi_{ij,k} = 1, \quad i = 1, \dots, N,$$

$\pi_{ij,k}$  is the transition probability from CF  $m_i$  to CF  $m_j$ . At the same time the unknown geometric parameters of the manipulated object and of the environment are estimated.

## 3 State and measurement equations

The system equation describes the positions and orientations of the manipulated object and the environment and it is linear. The different CFs are described by several nonlinear measurement models [3, 8].

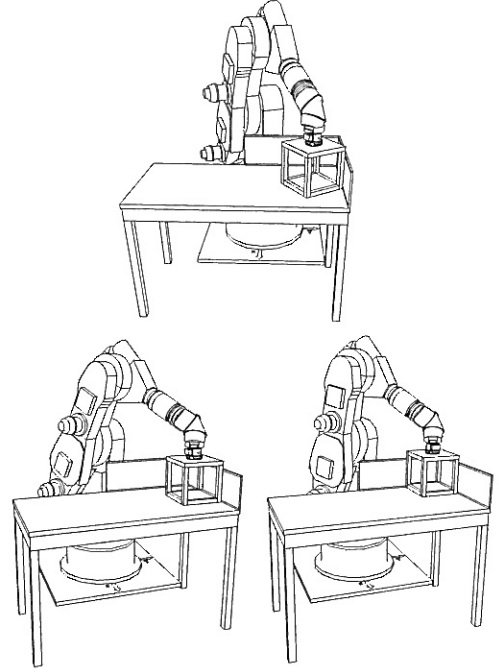


Figure 1: Robot placing a cube in a corner

**State equation.** The system model is of the form

$$x_{k+1} = x_k + \eta_k. \quad (3)$$

The estimated states are geometric grasping and environment parameters. The state vector comprises a part  $x_k^m$ , referring to the manipulated object, and a part  $x_k^e$  referring to the environment. Four reference frames are considered (Fig.2):  $\{w\}$  is the world frame,  $\{g\}$  is a frame placed on the gripper whose position and orientation

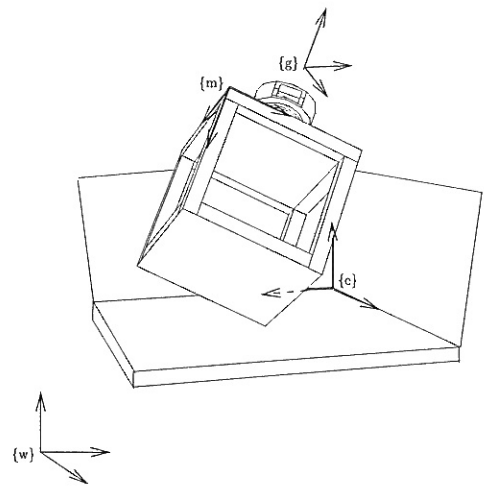


Figure 2: Frames

with respect to the world frame  $\{w\}$  are exactly known (through the position kinematics of the robot),  $\{m\}$  is a frame attached to the manipulated object, and  $\{e\}$  is a frame fixed with respect to the environment.

**Measurement equation.** The sensor measurements are translational and angular end-effector velocities,  $v_k$  and  $\omega_k$ , together with contact forces and moments,  $f_k$  and  $m_k$ , measured by a force/torque sensor. They are grouped in the *twist*  $t_k = (v_k^T, \omega_k^T)^T$ , *wrench*  $w_k = (f_k^T, m_k^T)^T$  and measurement  $z_k = (t_k^T, w_k^T)^T$  vectors. Measurement equations are derived for each CF from the reciprocity condition [3]. This condition states that any twist of the manipulated object is reciprocal to any wrench of the modelled wrench space (spanned by the basis  $G_i$ ) and that any wrench is reciprocal to any twist of the modelled twist space (spanned by the basis  $J_i$ ). Index  $i$  refers to the  $i$ -th CF. Then Eq. (2) acquires the form

$$h_{i,k} = \begin{pmatrix} G_{i,k}^T(x_{i,k}) t_k \\ J_{i,k}^T(x_{i,k}) w_k \end{pmatrix} = 0. \quad (4)$$

Both  $G_i$  and  $J_i$  contain trigonometric functions (sines and cosines) of the estimated states, such that the measurement functions [8] are nonlinear. To every CF correspond different twist and wrench bases. The models in Eq. (4) are very distinct, which is appropriate for using the multiple-model approach to solve the problem. Equation (4) is linearized for each CF around the current predicted state estimate  $\hat{x}_{i,k+1/k}$ . For the computation of the derivative of  $h_{i,k}$  with respect to the estimated variables, the partial derivatives of  $J_{i,k}$  and  $G_{i,k}$  are needed (See the Appendix).

**Closure equations.** The occurrence of a CF gives additional information on the state variables. The so-called kinematic closure equations [3]

$$c_i(x_{i,k}) = 0 \quad (5)$$

describe additional nonlinear constraints that relate different configuration variables (of the manipulated object and the environment) for each CF. The closure equations are models of the contacts obtained as a composition of basic contacts (vertex-face and edge-edge) between polyhedra. For instance, the *edge-face* contact between the cube and the environment is described by means of two vertex-face contacts, and the contact between two faces of the object is described as a composition of three vertex-face contacts, and so on.

For each CF, the closure equation is applied once. Its corresponding EKF uses as initial state estimate and estimation covariance matrix the ones obtained from the EKF based on the measurement equation. The state estimate and its estimation covariance matrix, computed by the closure equations are given to the interacting step of the IMM algorithm.

## 4 IMM estimator for transition and CF monitoring

The number of possible CFs between the manipulated object and the environment is in general high [5]. A set of mutually *exclusive* and *exhaustive* hypotheses is constructed to describe all possible CFs of the manipulated object from one place to another. For the case in which the manipulated object is a cube and the environment is a corner this number is 249 [11]. In the planner [11], a graph is constructed which nodes correspond to the possible CFs and its arcs to the transitions between them. Given the path of the motion and the level of uncertainty about the geometric parameters, it is possible to eliminate from the set of hypotheses those CFs whose distance  $d$  from the nodes of the path is higher than a given threshold  $d_{max}$  [12]. The distance  $d$  is the minimum number of arcs of the CF graph that are between two nodes. In this way a relevant amount of CFs can be eliminated [2, 5] and the number of hypotheses considerably reduced. Here it is assumed that the hypothesis  $H_0$  corresponds to the case of completely constrained object. Hypotheses  $H_i, i = 1, \dots, N$  describe all other CFs. With the models for each CF and its EKFs, an IMM estimator is implemented. So, the CFs can be monitored on-line, using the information provided by the IMM mode probabilities.

The nonlinear character of the measurement equations requires the use of EKFs or other nonlinear filtering techniques, such as [6] which needs no computation of derivatives. The present work estimates the state vectors through EKFs. Each EKF is of the form

$$\hat{x}_{i,k+1/k+1} = \hat{x}_{i,k+1/k} + K_{i,k+1} \nu_{i,k+1}, \quad (6)$$

$$\hat{x}_{i,k+1/k} = \hat{x}_{i,k/k}, \quad (7)$$

$$P_{i,k+1/k} = P_{i,k/k} + Q_{i,k}, \quad (8)$$

$$K_{i,k+1} = -P_{i,k+1/k} H_{x_{i,k+1}}^T S_{i,k+1}^{-1}, \quad (9)$$

$$P_{i,k+1,k+1} = \Gamma_{i,k+1} P_{i,k+1/k} \Gamma_{i,k+1}^T + K_{i,k+1} R_{i,k+1} K_{i,k+1}^T, \quad (10)$$

$$S_{i,k+1} = R_{i,k+1} + H_{x_{i,k+1}} P_{i,k+1/k} H_{x_{i,k+1}}^T, \quad (11)$$

where

$$\Gamma_{i,k+1} = I + K_{i,k+1} H_{x_{i,k+1}},$$

$$R_{i,k+1} = D_{i,k+1} R_{z,k+1} D_{i,k+1}^T,$$

$$H_{x_{i,k+1}} = \partial h_i / \partial \hat{x}_{i,k+1/k}, \quad D_{i,k+1} = \partial h_i / \partial z_{k+1},$$

$$\nu_{i,k+1} = h_i(\hat{x}_{i,k+1/k}, z_{k+1}).$$

$\hat{x}_{i,k+1/k+1}$  and  $\hat{x}_{i,k+1/k}$  are, respectively, the filtered and predicted state vectors,  $K_{i,k+1}$  is the EKF gain matrix,  $P_{i,k/k}$  is the estimation error covariance matrix,  $\nu_{i,k+1}$  is a "pseudo-innovation" process [9] and  $S_{i,k+1}$  its covariance matrix.  $I$  denotes the identity matrix. The estimated state vector is a probabilistically weighted sum of the state

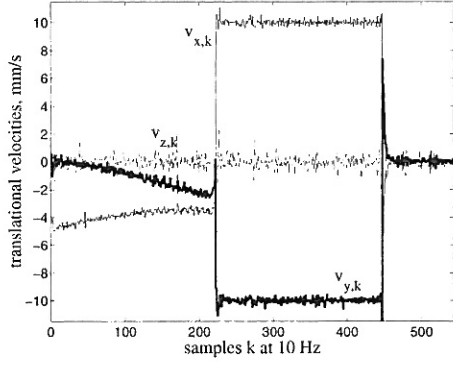


Figure 3: Measured translational velocities

estimates from the EKFs working in parallel, weighted by the IMM mode probabilities  $\mu_{i,k+1}$ , [1] i.e.

$$\hat{x}_{k+1/k+1} = \sum_{i=1}^N \mu_{i,k+1} \hat{x}_{i,k+1/k+1}, \quad (12)$$

where  $N$  is the number of the filters run in parallel.

## 5 Performance analysis on a cube-in-corner assembly

The proposed approach is applied to a cube-in-corner assembly system (Fig. 1). The experimental data are obtained with a KUKA-IR 361 industrial robot. The cube is mounted directly on the robot without flexibility between them. The measurements are taken at a frequency of 10 Hz. The experimental data (Figs. 3-6) correspond to the three CFs of the cube-in-corner assembly (Fig. 1):  $k \in [0, 220]$  is the face-face and edge-face contact,  $k \in [221, 450]$  is the two face-face contact, and  $k \in [450, 545]$  is the three face-face contact (completely constrained case). In the test a path with three CFs is used. In the IMM  $H_0$  is the hypothesis for three face-face contact,  $H_1$  for two face-face contact, and  $H_2$  for face-face and edge-face contact. The noise covariance matrices  $Q$  and  $R_z$

$$Q = \text{diag}(5, 5, 5, 0.001, 0.001, 0.001, \\ 1, 1, 1, 0.001, 0.001, 0.001),$$

$$R_z = \text{diag}(0.050, 0.4, 1.96, 4 \cdot 10^{-7}, 5 \cdot 10^{-6}, 9 \cdot 10^{-8}, \\ 0.060, 0.009, 0.008, 150, 87, 51)$$

are the same for all EKFs. The units of the elements of  $Q$  are  $mm^2$  and  $rad^2$ , respectively for the positions and angles, and those of  $R_z$  are  $(mm/sec)^2$ ,  $(rad/sec)^2$ ,  $N^2$ ,  $(Nmm)^2$  for the measured velocities, forces and moments. The system noise covariance matrix  $Q$  reflects the presence of linearization errors, whereas the measurement noise

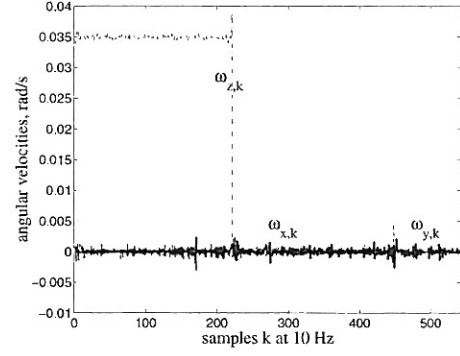


Figure 4: Measured angular velocities

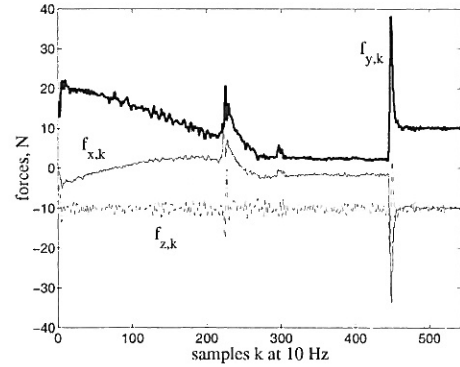


Figure 5: Measured forces

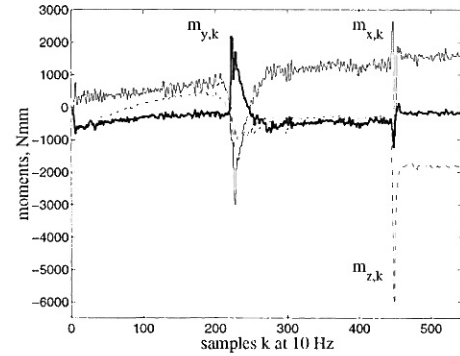


Figure 6: Measured moments

covariance is known for the used sensors. The IMM transition probability matrix, and the initial probability vector are chosen as follows:

$$Pr = \begin{pmatrix} 0.98 & 0.01 & 0.01 \\ 0.01 & 0.98 & 0.01 \\ 0.01 & 0.01 & 0.98 \end{pmatrix}, \mu_0 = \begin{pmatrix} 1/3 \\ 1/3 \\ 1/3 \end{pmatrix}$$

Due to the lack of information, equal initial probabilities are assumed for the different CFs.

It is clear from Fig. 8 that by the IMM probabilities the contact transitions can be detected on time. After the change a small period is needed and the algorithm resolves the "competition" between the CFs. This is reflected also in the Normalized Innovation Squared (NIS) test  $\epsilon_k = \nu_k S_k^{-1} \nu_k$  [1] (Fig. 7) and in the peak estimation errors. In the periods of transitions the estimates are not reliable.

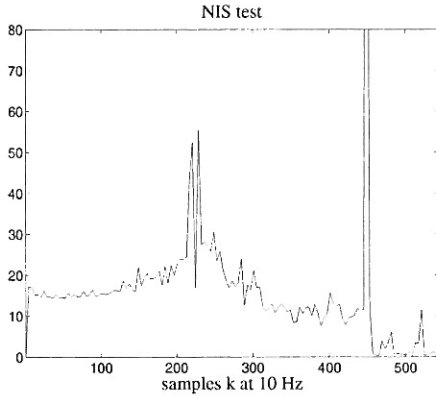


Figure 7: NIS test

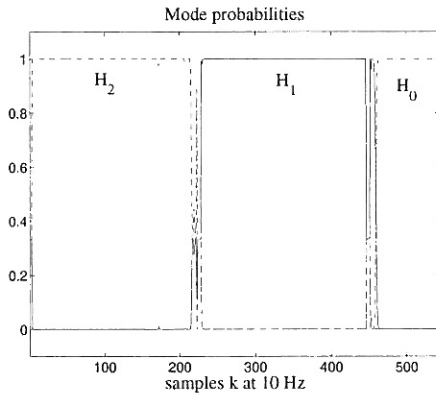
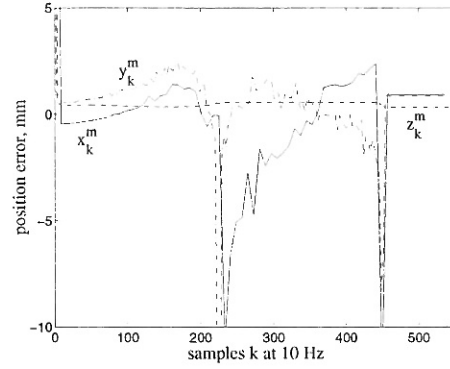
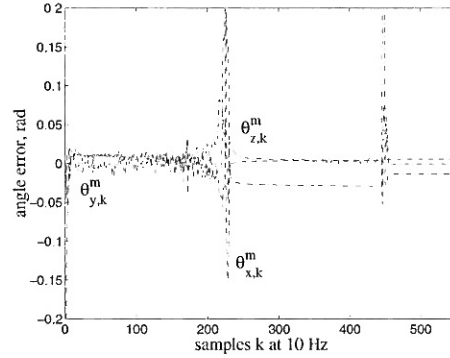
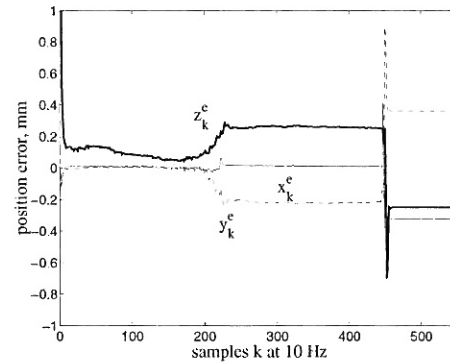


Figure 8: IMM mode probabilities

The estimation error  $e_k = \hat{x}_{k/k} - x_k$  of the positions and orientations is presented in Figs. 9-12. The true values of the estimated states are:  $x^m = 125 \text{ mm}$ ,  $y^m = 125 \text{ mm}$ ,  $z^m = -110 \text{ mm}$ ,  $\theta_x^m = 0 \text{ rad}$ ,  $\theta_y^m = 0 \text{ rad}$ ,  $\theta_z^m = -0.7854 \text{ rad}$ ,  $x^e = 440 \text{ mm}$ ,  $y^e = -600 \text{ mm}$ ,  $z^e = -750 \text{ mm}$ ,  $\theta_x^e = 0 \text{ rad}$ ,  $\theta_y^e = 0 \text{ rad}$ ,  $\theta_z^e = 3.1416 \text{ rad}$ . The NIS test (Fig. 7) and the mode probabilities (Fig. 8) contain information about the type and instants of contact transitions. By the IMM approach the CFs and the transitions between them are detected on-line and at the same time the unknown parameters of the manipulated object and the environment are estimated. So, both modes detection and estimation are performed automatically. Of course, the computational cost is proportional to the number of the EKFs (CFs). The IMM filter, implemented

Figure 9: Error  $e_k$  in positions of the cubeFigure 10: Error  $e_k$  in orientation angles of the cubeFigure 11: Error  $e_k$  in positions of the environment

in the present paper, is with a fixed structure. When the estimation block is connected with the planning part [5, 11, 12], the estimator can receive from the graph of the planner information about the next neighboring CFs. Based on this graph structure of the CFs, variable structure IMM algorithms can be designed. Extensions to cases with time-varying geometric parameters of the manipulated object and the environment can be performed in a similar way.

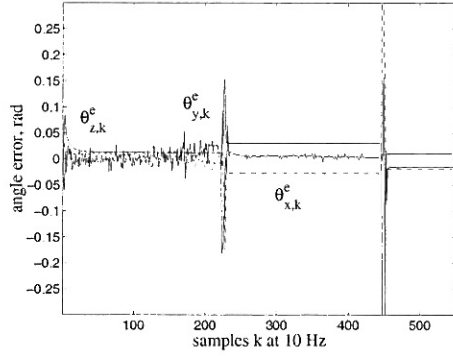


Figure 12: Error  $e_k$  in angles of the environment

## 6 Conclusions

In this paper a general approach to contact transitions detection and estimation of uncertain geometric parameters (positions and orientation angles) is proposed for force-controlled robotic tasks in which a robotic manipulator moves an object in contact with the environment, both rigid and polyhedral.

The different CFs are described by different nonlinear measurement equations, whereas the system equation is linear. An IMM estimator is implemented and its performance is evaluated by real sensor data (linear and angular velocities, forces and moments). The IMM probabilities and the normalized innovation squared test permit to monitor the occurring CFs. The experimental assembly of moving a cube into a corner demonstrates high estimation accuracy and quick detectability of the contact transitions.

## Appendix

**Derivatives Computation.** The computation of the measurement and closure equations is based on the screw-transformation matrices [3], that are functions of the rotation matrices between the different frames [3, 4]. The partial derivatives are found from Eq. (4) and have the form

$$\frac{\partial h_{i,k}}{\partial x_{i,k}} = \begin{pmatrix} \partial(G_{i,k}^T(x_{i,k}))/\partial x_{i,k}^{mT} & \partial(G_{i,k}^T(x_{i,k}))/\partial x_{i,k}^{eT} \\ \partial(J_{i,k}^T(x_{i,k}))/\partial x_{i,k}^{mT} & \partial(J_{i,k}^T(x_{i,k}))/\partial x_{i,k}^{eT} \end{pmatrix},$$

$$D_{i,k} = \partial h_{i,k}/\partial z_k = \begin{pmatrix} G_{i,k}^T & 0 \\ 0 & J_{i,k}^T \end{pmatrix}.$$

The matrix derivatives are computed according to the rules for matrix calculus operations [10].

**Acknowledgments** H. Bruyninckx and T. Lefebvre are, respectively, Postdoctoral and Doctoral Fellow of the Fund for Scientific Research–Flanders (F.W.O) in Belgium. Financial

support by the Belgian Programme on Inter-University Attraction Poles initiated by the Belgian State – Prime Minister’s Office – Science Policy Programme (IUAP), the F.W.O. under grant G.0295.96N, and K.U.Leuven’s Concerted Research Action GOA/99/04 is gratefully acknowledged.

## References

- [1] Y. Bar-Shalom and X. R. Li, *Estimation and Tracking: Principles, Techniques and Software*, New York, Artech House, 1993.
- [2] H. Bruyninckx, T. Lefebvre, L. Mihaylova, E. Staffetti, J. De Schutter and J. Xiao, A Roadmap on Autonomous Robotic Assembly, *Proc. of the Int. Symp. on Assembly and Task Planning*, Fukuoka, Japan, 2001.
- [3] J. De Schutter, H. Bruyninckx, S. Dutré, J. De Geeter, J. Katupitiya, S. Demey and T. Lefebvre, Estimating First-Order Geometric Parameters and Monitoring Contact Transitions During Force-Controlled Compliant Motions, *Int. J. Robotics Res.*, Vol. 18, No. 12, pp. 1121-1184, 1999.
- [4] J. De Schutter and H. Van Brussel, Compliant Robot Motion, I, II, *Int. J. Robotics Res.*, Vol. 7, No. 4, pp.3-33, 1988.
- [5] X. Ji and J. Xiao, Automatic Generation of High-Level Contact State Space, *Proc. of the 1999 IEEE Intern. Conf. on Robotics and Automation*, pp. 238-244, 1999.
- [6] S. Julier, J. Uhlman and H. Durrant-Whyte, A New Method for the Transformation of Means and Covariances in Filters and Estimators, *IEEE Trans. on Automatic Control*, Vol. 45, No. 3, pp. 477-482, 2000.
- [7] T. Lefebvre, H. Bruyninckx and J. De Schutter, Estimation and Propagation of Uncertainties During Force-Controlled Execution of Contact Formation Sequences, *Proc. of the 10-th Int. Conf. on Advanced Robotics*, Hungary, 2001.
- [8] T.Lefebvre, H. Bruyninckx, and J. De Schutter, Estimation of Geometrical Parameters During Force-Controlled Execution of Polyhedral Contact Formation Sequences, *Internal Report 2001ROO5*, K.U.Leuven, Belgium, 2001.
- [9] S. Soatto, R. Frezza and P. Perona, Motion Estimation via Dynamic Vision, *IEEE Trans. on Automatic Control*, Vol.41, No. 3, pp. 393-414, 1996.
- [10] W. Vetter, Matrix Calculus Operations and Taylor Expansions, *SIAM Review*, Vol. 15, pp. 352-369, 1973.
- [11] J. Xiao and X. Ji, A Divide-And-Merge Approach to Automatic Generation of Contact States and Planning of Contact Motions, *Proc. of the 2000 IEEE Intern. Conf. on Robotics and Automation*, 2000.
- [12] J. Xiao and L. Zhang, Towards Obtaining All Possible Contacts - Growing A Polyhedron by its Location Uncertainty, *IEEE Trans. on Robotics and Automation*, Vol. 12, No. 4, pp. 553-565, 1996.